Article citation info:
Czarnigowski J, Trendak M. Aircraft piston engine load distribution in steady state operating conditions. Combustion Engines. 2023; 193(2):29-35. https://doi.org/10.19206/CE-160505

Jacek CZARNIGOWSKI
Michał TRENDAK

Combustion Engines
Polish Scientific Society of Combustion Engines

Aircraft piston engine load distribution in steady state operating conditions

ARTICLE INFO

Received: 29 September 2022
Revised: 3 January 2023
Accepted: 3 February 2023
Available online: 13 February 2023

The article presents the results of statistical analysis of aircraft piston engine operational parameters during normal operating conditions. Test was carried out on ultralight gyroplane Tercel produced by Aviation Artur Trendak equipped with CA 912 ULT piston engine. Research was conducted under normal operating conditions of the autogyro and data was collected from 15 independent tests including a total of 14 flight hours conducted during training flights. Engine and flight parameters were recorded at 9 Hz during each flight using on-board Flight Data Recorded system. The data collected was subjected to statistical analysis to determine the statistical distribution of parameters defining the engine's operating condition. The analysis covered engine speed, intake manifold pressure, oil temperature, head temperature and exhaust gas temperature. The results were presented in the form of histograms showing the characteristic ranges of the parameters in aviation engine operation. An analysis of the rate of change of the analysed parameters was then carried out. This was the basis for defining the engine's steady state. The results showed that the steady state of the engine under these operating conditions accounted for more than 78% of the total engine operating time. A Power Consumption Ratio indicating the load range of the engine was determined for steady states. It was shown that most of the time the motor operates at an average load of between 50% and 80% of the nominal value.

Key words: *piston engine, engine parameters, statistic, normal operating conditions*

1. Introduction

Aviation continues to be one of the leading industries and a driver of innovation [1]. The main directions of aviation development are to increase the safety of the structure and its operation, and to increase its efficiency, defined as the energy consumption to transport the load. This is particularly important in the case of the fastest growing branches of aviation is ultralight aviation, i.e. small, maximum two-seat aircraft with take-off mass not exceeding 600 kg [2–4]. These are aircraft that can be used from short grass airfields, significantly increasing their availability for recreational and utility use. In addition, the regulations to which they are subject significantly simplify the requirements for their use and maintenance, allowing low operating costs [5].

Modern technologies are widely used in ultralight aircraft. Simplified construction certification procedures allow modern solutions to be introduced into their design much more quickly than in General Aviation or Transportation Aviation [6]. The use of modern materials, such as carbon fiber, allow a reduction in empty weight, therefore increasing the payload weight [2, 7, 8]. The use of modern materials also allows the shapes of the aircraft themselves to be optimized, thereby increasing their aerodynamic efficiency [9]. This makes it possible to reduce energy requirements or increase cruise speeds [10, 11].

Optimization also extends to powertrains. For ultralight aircraft, the main propulsion system currently used is a small piston engine. They are characterized by construction simplicity, low failure rate and low weight [12, 13]. The development of that engines is mainly aimed at increasing the power-to-weight ratio. It is done by minimize the size of the engine components and reduce of its weight without changing the power or by increase power while maintaining or slightly increasing the weight of the engine. A common solution is the turbocharging systems [14] which allows to obtain higher power at similar weight. However it leads to increase of the thermal and mechanical load of the engine [15]. This requires increased attention in operation and maintenance.

The best solution would be to combine both methods or to introduce a new type of power unit that meets the criteria of a higher power-to-weight ratio than at present. This leads to ideas of using electric or hybrid systems [16–18]. Such systems have been well introduced in automotive propulsion systems [19].

In both cases, the optimization of current propulsion systems and the introduction of new ones requires the gathering of data on the range and operating conditions of these units under actual operating conditions. This is because the conditions of operation, particularly the load range of the engine and the steady-state and transient operation ratio, strongly influence the stresses on the structures and their lifetime [20–22]. However, these data cannot be translated between different types of vehicle, and especially between motor vehicles and aircraft.

The authors of the work [19, 23], highlighting the significant contribution of dynamic states under normal vehicle operating conditions. They show that dynamic conditions occupy from 20% to 50% [19]. For aircraft engines, the contribution of dynamic conditions is much smaller [16] and do not across ranges from 5% to 20% of the engine operating time [17]. The difference also are shown in the

average conditions of steady state engine operation. In the vehicles, the average conditions correspond to about 20% to 30% of the nominal power [1], while in the case of aircraft engines, they are much higher, about 50 to 70% [17, 24]. Knowledge of the exact distribution of operating parameters is therefore important for the development of propulsion systems.

This paper presents an analysis of performance of CA 912 RSTi engine, used to propel the Tercel autogyro in real operating conditions.

2. Methodology and research object

2.1. Research object

The research was carried out on a autogyro with registration number SP-XXBX type Tercel, produced by Aviation Artur Trendak. It is a two-seat ultralight autogyro, designed for recreational, training, commercial use and sport. The Tercel autogyro is shown in Fig. 1. Basic technical data of the tested autogyro are shown in Table 1.

Fig. 1. Test object: Tercel autogyro produced by Aviation Artur Trendak

Table 1. Technical data of Tercel autogyro [25]

Dimensions		
Rotor diameter	8.60	m
Rotor disc area	60.82	m^2
Rotor blade chord	0.20	m
Overall length (without rotor)	5.04	m
Hull width	2.35	m
Cabin width	2.20	m
Cabin width	1.36	m
Overall height	2.35	m
Wheel diameter	2.87	m
Weight		
Maximum take-off weight	560	kg
Empty weight	295	kg
Payload weight	265	kg
Propulsion System		
Engine gear ratio	1:2.43	
Propeller diameter	1.72	m
Propeller	Kaspar Aero 2/3 LT	
Fuel tank capacity	120	l

The Tercel is powered by a CA 912 RSTi engine. It is four cylinder boxer type engine, turbocharged with electronic injection system. The technical data of the CA 912 ULT engine are shown in Table 2.

Table 2. Technical data of CA 912 ULT engine [25]

Parameter	Value
Cylinder no.	4, boxer
Displacement	1211 cm^3
Cylinder diameter	79.5 mm
Piston stroke	61 mm
Compression ratio	9.0:1
Engine gear ratio	2.43:1
Fuelling system	Indirect, multipoint injection system Auris by Auto&Aero Technologies
Turbocharging	Turbocharger with an exhaust gas pressure control valve
Take-off power	140 HP (at 5800 rpm)
Nominal power	125 HP (at 5500 rpm)
Idle speed	2000 rpm

2.2. Scope of research

The aim of the study was to analyse the statistical distributions of the main parameters of the aircraft engine operation in real operating conditions in steady and transient state. The data was collected by Flight Data Recorder FDR K.01 produced by Auto&Aero Technologies Sp. z o.o. and built into the autogyro as standard equipment. FDR collects the information from the avionics system and the engine control system via RS485 communication (Fig. 2).

Fig. 2. Flight Data Recorder used in the research

The tests were conducted from 19.10.2021 to 28.10.2021 in Baranów airbase. There were 20 independent tests (flights) during pilots training flights – Table 3. These flights included mainly full Airfield traffic pattern with full landing or touch-and-go. In 4 cases these were navigational distance flights. The time to take one Airfield traffic pattern was about 8 to 15 minutes and the time for a single recording (single flight) ranged from 22 to 90 minutes. In total, the flights covered 1009 minutes and 88 take-offs and landings.

During the flights, the following parameters, among others, were recorded at 9 Hz:

- Air speed, km/h;
- Altitude, m. asl;
- Climb rate, m/s;
- Rotor speed, rpm;
- Crankshaft speed, rpm;
- Intake manifold pressure, kPa;
- intake manifold air temperature, °C;

– fuel pressure, kPa;
– oil pressure, kPa;
– oil temperature, °C;
– 2 × head temperature, °C;
– 2 × exhaust temperature, °C.

Table 3. Test flights

No	Date	Duration, min	Landings
1	19.10.2021	65	8
2	19.10.2021	35	4
3	19.10.2021	60	8
4	19.10.2021	88	8
5	20.10.2021	58	1
6	20.10.2021	22	2
7	20.10.2021	65	7
8	20.10.2021	64	7
9	21.10.2021	60	5
10	22.10.2021	19	1
11	26.10.2021	61	6
12	26.10.2021	57	6
13	26.10.2021	58	1
14	26.10.2021	58	4
15	27.10.2021	38	4
16	27.10.2021	36	2
17	27.10.2021	61	2
18	27.10.2021	33	4
19	28.10.2021	34	4
20	28.10.2021	37	4
	Total	**1009**	**88**

2.3. Methodology

The collected data were subjected to statistical analysis. For each parameter, an occurrence histogram was determined. In the case of speed and intake manifold pressure, a histogram of the occurrence of the dependence on these two variables was also determined.

The next step was a steady-state and transient analysis. For this purpose, an analysis of the rate of change of the analyzed parameters was carried out. According to the literature [15, 18, 26], it was assumed that steady state can be defined as such a state of engine operation in which the rate of parameters defining the operating point does not change by more than 1% of range per second. On this basis, steady-state operating points were determined. The parameters considered in this case are engine speed, manifold air pressure and the thermal state of the engine expressed by oil temperature and head temperature. The stability of all 4 parameters together define the steady-state operating point of the engine.

For such a defined steady-state operating point, a load distribution analysis of the engine was carried out. The engine load (P_{CR} – power consumption ratio) was determined as a relative value:

$$P_{CR} = \frac{n_i - n_{idle}}{n_{nom} - n_{idle}} \cdot \frac{MAP_i - MAP_{idle}}{MAP_{nom} - MAP_{idle}} \quad (1)$$

where: n_i – engine speed at the analysed point; MAP_i – manifold air pressure at the analysed point; n_{nom} – engine speed at the nominal power (5500 rpm); MAP_{nom} – manifold air pressure at the nominal power (135 kPa); n_{idle} – engine speed at the idle (1800 rpm); MAP_{idle} – manifold air pressure at the idle (30 kPa).

The value of the defined coefficient is defined in the range of engine operation from idle (value 0) to nominal power (100%). When the engine is operating at take-off power, the coefficient value will be greater than 100%. This approach is in line with the definition of engine load in the aircraft engine certification specification. The values corresponding to idle and rated power were determined from the engine manufacturer's data.

The above analyses were carried out for all flights together. The results were presented as histograms of the distribution of the analysed parameters.

3. Analysis of results

Figure 4 shows the distribution of engine operating point rates during tests. The operating points are defined by engine speed and manifold air pressure. Two groups of operating points can be seen: the idle range (n = 1500–2000 rpm and MAP = 20–40 kPa) and the engine load (n = 4000–6000 rpm and MAP = 70–140 kPa). The highest frequent engine operating points occur at idle for 1500–2000 rpm and intake manifold pressure 30–40 kPa and their rate is 28.3%. In the case of engine loads during normal flight, the frequency is 55.5% and occurs at 4000–5400 rpm and MAP = 80–120 kPa. The distribution of points is fairly uniform over this range, with the highest frequency occurring at 5000 rpm and MAP = 115 kPa and equal to 5.4%. There is also a significant occurrence of the engine starting power (n = 5500–6000 rpm and MAP = 120–140 kPa) amounting to 5.1% in the studied flights. This power is used during takeoffs and the climb after take-off. A very small proportion of intermediate conditions is also evident.

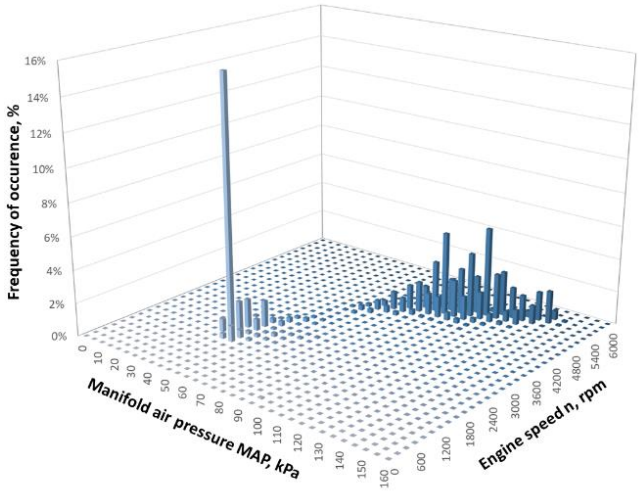

Fig. 4. Distribution of engine operating points during flights

This is more visible if we look at the distribution obtained as a map of the occurrence of work points. Figure 5 shows this distribution, assuming that the size of the circle at a given operating point corresponds to its frequency of occurrence. It can be seen that most of the working points are concentrated along one line – the propeller characteristic (marked in Fig. 5 by the line). This is a characteristic distribution for the cooperation of the engine with the propeller with constant characteristics. The concentration of

operating points in the idle, flight and take-off and climb (TOGA) range, as described earlier, is also visible.

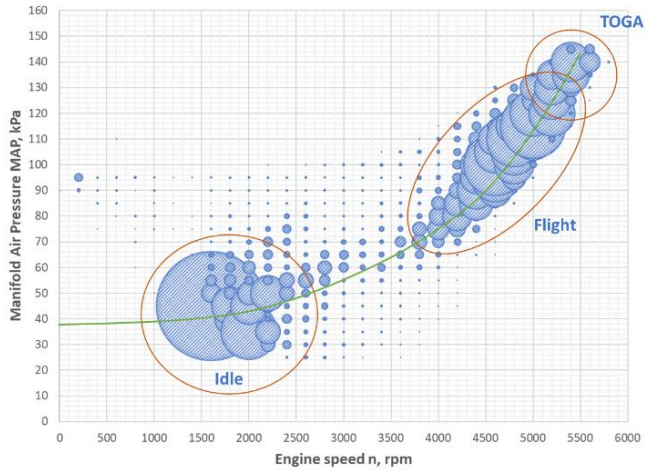

Fig. 5. Distribution of engine operating points during flights

Next the analysis was performed only for engine speed (Fig. 6) and separately for manifold air pressure (Fig. 7). For the flights, the highest frequency of occurrence was a speed around 1600 rpm corresponding to engine idle. The engine operated at this speed 17.0% of the total engine run time. The second most common speed range is around 4800 rpm. The 4600–4800 rpm range is 25.8% and the 4800–4500 rpm range is 20.1%. These ranges correspond to a cruising power of about 50% to 80% of the nominal power of the engine. The speed range 2000–2400 rpm, corresponding to the engine warm-up process, is also a significant part of the engine work and occupies a total of 12.3%. This is due to short single flights, for which the warm-up time is a significant part.

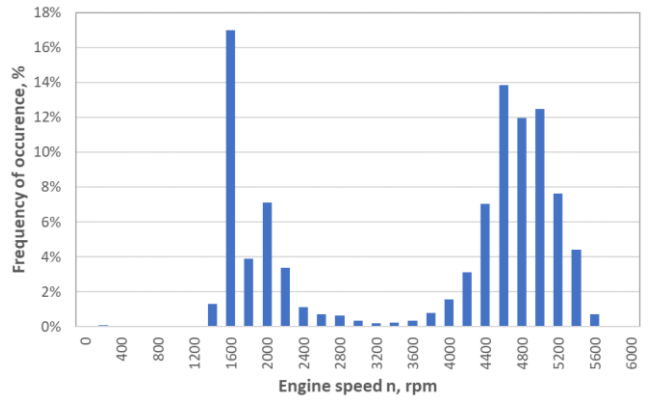

Fig. 6. Distribution of engine speed during flights

Similar distributions are seen in the manifold air pressure (MAP) (Fig. 7). The most common pressure is the range 40–50 kPa corresponding to engine idle. This occurs for 19.7% of the engine operating time. The MAP ranges from 100 kPa to 120 kPa occur with a similar frequency of about 5–8% for each 5 kPa interval considered.

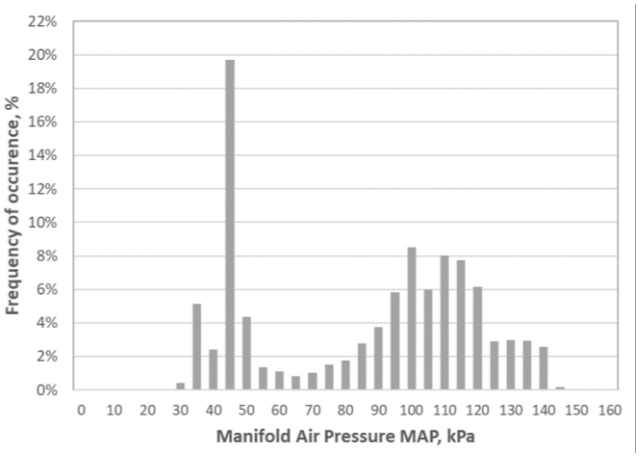

Fig. 7. Distribution of manifold air pressure during flights

Another group of analyses concerns temperatures. One of the important temperatures during engine operation is the oil temperature. Among other things, this is used as a basis for the decision to start (according to the operating manual, the oil temperature must exceed 60°C). As shown in Figure 8, the oil temperature is quite stable and after the engine warm-up was maintained in the range of 70°C to 86°C. It can be seen that the warm-up period accounted for a total of 7.3% of the total engine running time (temperatures below 62°C).

A similar stability can be observed by analysing the temperature of the cylinder heads (Fig. 9). Both sides of the engine maintain a similar temperature between 64°C and 84°C for more than 85% of the engine running time.

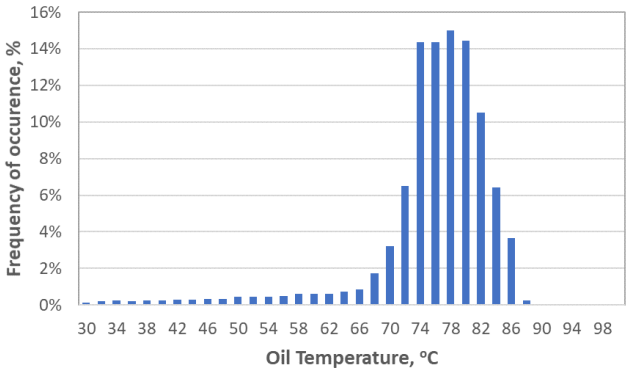

Fig. 8. Distribution of oil temperature

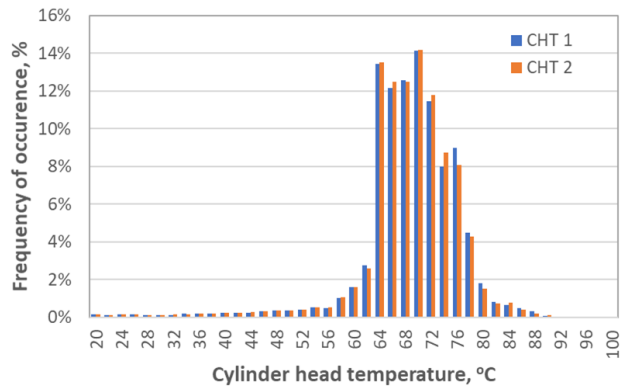

Fig. 9. Distribution of cylinder heads temperature

Similar to oil, the warm-up time (reaching 60°C) is a total of 8.0% of the engine operating time. It should be noted here that the stability of these temperatures is also related to the installation of the engine on the airframe and the proper heat dissipation from the oil and engine coolant cooling systems.

The distribution of exhaust gas temperatures (Fig. 10) shows a very high stability in the engine's operation under load. temperatures are maintained in the range of 760°C to 820°C for more than 65.3%. At lower loads, however, a significant difference in the temperature distribution for both sides of the engine (EGT 1 and EGT 2) is apparent. In this case, the right side of the engine (EGT 1) maintained about 150°C higher gas temperatures than the left side (ETG 2). This is a common case in these engines resulting from both combustion irregularities. Once the temperature exceeds 750°C (corresponding to about 50% of the nominal power), this difference practically disappears.

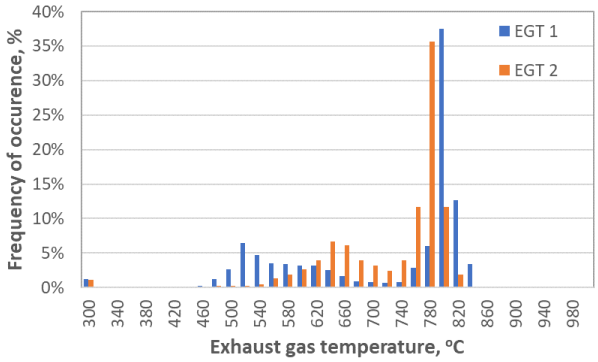

Fig. 10. Distribution of exhaust gases temperature

Another analysis included the rate of change of engine speed (Fig. 11). For analysed flights, more than 85% of the operating time is stable conditions in which the rate of change of engine speed does not exceed ±50 rpm/s. Rate of change higher than ±150 rpm/s is only 2.6% (symmetrically 1.3% decrease and increase of speed). These values are due to the landing (taking off the throttle before landing) and takeoff (rapid addition of throttle) stages. Assuming a 1% range/s limit of 58 rpm/s, it can be assumed that more than 87.5% corresponds to the steady state condition.

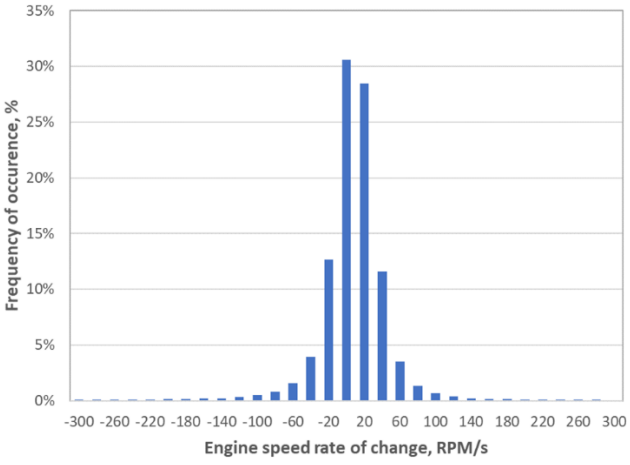

Fig. 11. Distribution of engine speed rate of change

The stability of engine operating conditions is even more apparent when the rate of change of manifold air pressure is analysed (Fig. 12). For analysed flights, the pressure practically does not change faster than ±3 kPa/s – 89.2%. Assuming a 1% range/s limit of 1.5 kPa/s, it can be assumed that more than 82.3% corresponds to the steady state condition. Maximal changes do not exceed ±9 kPa/s.

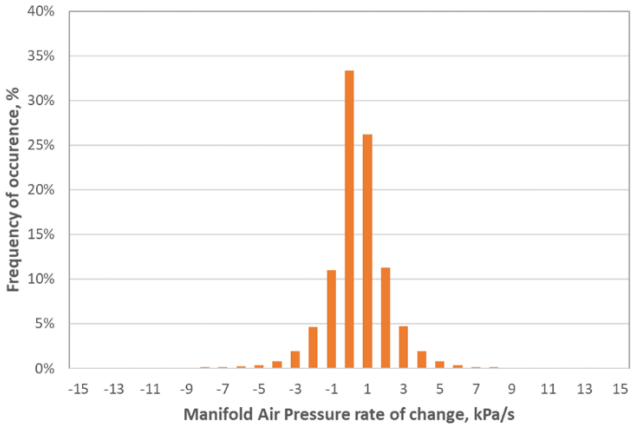

Fig. 12. Distribution of manifold air pressure rate of change

By analysing the rate of change of the oil temperature (Fig. 13), we can see that the rate of change is very low. The thermal capacity of the system causes most of the change to be in the range of ±0.2°C/s: over 87.9%. Taking 1% of the variation range kPa/s as the stability index (0.8°C/s), it can be assumed that 99.2% of the points meet the conditions for stable operation.

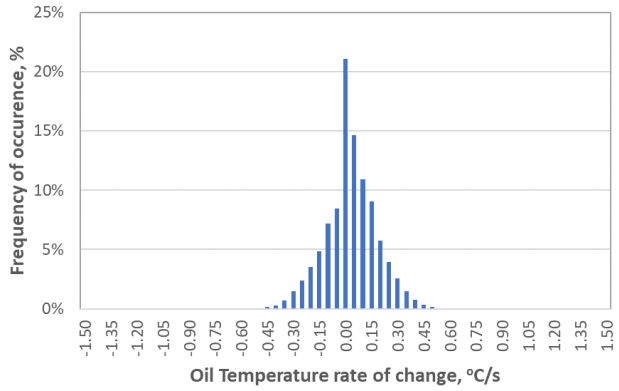

Fig. 13. Distribution of oil temperature rate of change

Similar results were observed for head temperatures (Fig. 14). Again, 99.4% of cases are within 1% (1°C/s). As for the oil, 91.7% of cases are within ±0.2°C/s. Thus, virtually all points meet the engine's steady-state condition.

On the basis of the assumed limits of engine dynamics, an analysis of engine operating states was carried out. The engine was assumed to operate as a steady state condition for four parameters: speed, intake manifold pressure, oil temperature and head temperature. On this basis, an analysis was carried out for the entire flight range. Figure 15 shows the results of the analysis. The vast majority of engine operation is at steady state: 78.9 %.

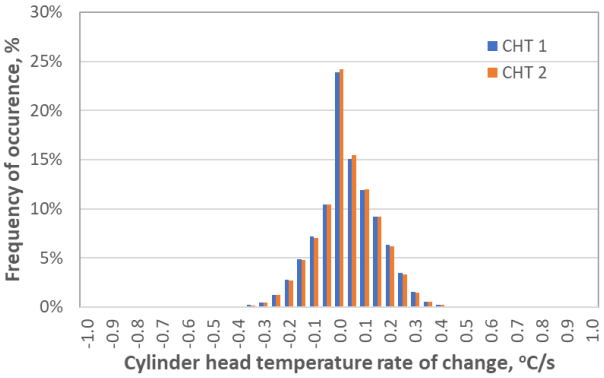

Fig. 14. Distribution of cylinder head rate of change

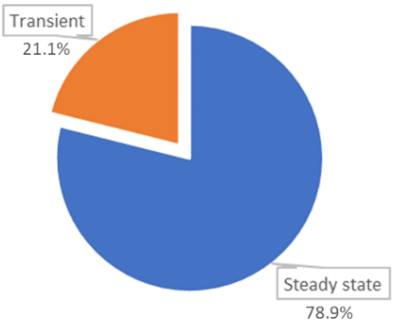

Fig. 15. Distribution of steady state and transient condition of engine work

The next step of the analyses was to analyse the Power Consumption Ratio distribution for steady-state engine operation (Fig. 16). It can be seen that idling is 18.6% and warming up (5% power) is 15.1%. The engine works very seldom in the power range between 10 and 45% of the nominal power and this applies mainly to transient conditions. The next range, covering about 55% of nominal power, is 7.8% and corresponds to stable flight at low cruise speed. Increasing speed causes an increase in power demand, which corresponds to further points in the range from 60 to 80% of nominal power. The distribution of occurrence here is quite constant and is for each range about 5 to 7%. Take-off power (above 100% nominal power) occurs a total of 3.3% of the time and nominal power 2.1%.

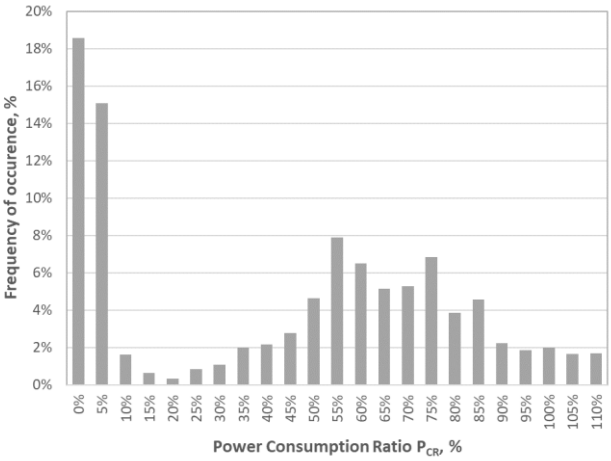

Fig. 16. Distribution of Power Consumption Ratio

Conclusions

The research shows that the aircraft engine operates in the vast majority of steady-state conditions. In the analysed flights, steady state was 78.9% of the total operating time. If we take into account that most of these flights were carried out as airport circle flights as part of pilot training, the dynamics in cruise flight use should be even lower. Changes in speed and air pressure in the intake manifold are mainly responsible for the transient. Variations in oil, head and exhaust gas temperatures are much smaller and mostly fall within the definition of steady state.

Aircraft engines operate at average high loads. During the flights, the most common operating condition was an engine load of 50–80% of nominal power – 55%. The second most frequent operating condition of the engine is idling (18.6%) and warming up (15.1%). Take-off power (above 100% nominal power) occurs a total of 3.3% of the time and nominal power 2.1%. Small engine loads (below 50%) practically did not occur during the research. Their share in the total engine operating time is marginal.

Bibliography

[1] Andrych-Zalewska M, Chłopek Z, Merkisz J, Pielecha J. Evaluation of the test drive cycle conditions impact on exhaust emissions from an internal combustion engine. Combustion Engines. 2018;175(4):3-9. https://doi.org/10.19206/ce-2018-401

[2] Czarnigowski J, Wendeker M, Jaklinski P, Nazarewicz A, Piertykowski K, Geca M, et al. Model of injection system for SI radial aircraft engine. SAE Technical Papers 2007-01-1903. 2007. https://doi.org/10.4271/2007-01-1903

[3] Markowski J. Correction of the model for assessing the emission of harmful exhaust emissions from the engine of a small aircraft during the flight. Transp Res Proc. 2018;35: 230-239. https://doi.org/10.1016/j.trpro.2018.12.025

[4] Bakholdin D, Biryukov V, Tolstobrova L. Determining parameters of electric power unit for light aircraft. AER Adv Eng Res. Proceedings of the International Conference Actual Issues of Mechanical Engineering (AIME 2018). 2018; (157):65-69. https://doi.org/10.2991/aime-18.2018.13

[5] Jakliński P, Wendeker M, Czarnigowski J, Duk M, Zyska T, Klimkiewicz J. The comparison of the operating parameters in an aircraft radial piston engine fuelled by 100LL and ES95 gasoline. Combustion Engines. 2009;136(1):52-59. https://doi.org/10.19206/CE-117220

[6] Czarnigowski J, Jakliński P, Zyska T, Klimkiewicz J. Analysis of influence of legal requirements on the design of electronic ignition system for aviation piston engine. Journal of Kones. 2017;24(1):91-100. https://doi.org/10.5604/01.3001.0010.2801

[7] Kwon H, Park Y, Shin C, Kim J-H, Kim C-G. In-flight strain monitoring of aircraft tail boom structure using a fiber bragg grating sensor based health and usage monitoring system. Int J Aeronaut Space. 2021;22(3):567-577. https://doi.org/10.1007/s42405-020-00324-0

[8] Zhu L, Li N, Childs PRN. Light-weighting in aerospace component and system design (2018) Propul Power Research. 2018;7(2):103-119. https://doi.org/10.1016/j.jppr.2018.04.001

[9] Rohani SV, Jahangirian A. A fast and efficient method for multiobjective aerodynamic optimization of a civil aircraft fuselage. J Aerospace Eng. 2022;35(6). https://doi.org/10.1061/(ASCE)AS.1943-5525.0001494
[10] Sabater C, Stürmer P, Bekemeyer P. Fast predictions of aircraft aerodynamics using deep-learning techniques. AIAA J. 2022;60(9):5249-5261. https://doi.org/10.2514/1.J061234
[11] Song C, Liu H, Zhou Z, Luo X, Li W. Inverse design of aerodynamic configuration using generative topographic mapping. Xibei Gongye Daxue Xuebao/Journal of Northwestern Polytechnical University. 2022;40(4):837-844. https://doi.org/10.1051/jnwpu/20224040837
[12] Shen Y-G, Nie K, Xu J-S, Chen G-S. Combustion and emission characteristics of compression-ignition aero piston engine at different altitudes. Tuijin Jishu/Journal of Propulsion Technology. 2022;43(4). https://doi.org/10.13675/j.cnki.tjjs.200896
[13] Zhao Z, Cui H. Numerical investigation on combustion processes of an aircraft piston engine fueled with aviation kerosene and gasoline. Energy. 2022;239:122264. https://doi.org/10.1016/j.energy.2021.122264
[14] Grabowski Ł, Karpiński P, Rudzik D. Study on operating load of the compression ignition engine. Combustion Engines. 2017;168(1):168-171. https://doi.org/10.19206/CE-2017-127
[15] Heywood JB. Internal Combustion Engine Fundamentals. McGraw Hill, New York, 1988.
[16] Bai M, Yang W, Song D, Kosuda M, Szabo S, Lipovsky P, Kasaei A. Research on energy management of hybrid unmanned aerial vehicles to improve energy-saving and emission reduction performance. Int J Env Res Pub He. 2020;17:2917. https://doi.org/10.3390/ijerph17082917
[17] Yuhimenko V, Baimel D. Sitbon M, Averbukh M, Lineykin S, Kuperman A. Hybrid internal combustion engine based auxiliary power unit. Micromachines. 2020;11:438. https://doi.org/10.3390/mi11040438
[18] Zhao X, Guerrero JM, Wu X. Review of aircraft electric power systems and architectures. Energycon 2014 – IEEE Int. Energy Conf. 2014:949-953. https://doi.org/10.1109/ENERGYCON.2014.6850540
[19] Song J, Cha J. Analysis of driving dynamics considering driving resistances in on-road driving. Energies. 2021;14: 3408. https://doi.org/10.3390/en14123408
[20] Bieniek A, Brol S, Mamala J. The system for estimation parameters of internal combustion engine in the road test. Journal of Kones. 2011;18(2):279-286.
[21] Sureshkumar J, Venkitachalam G, Mallikarjuna JM, Elayaraja R. Study on effect of engine operating parameters on flame characteristics. SAE Technical Papers 2015-01-0749. 2015. https://doi.org/10.4271/2015-01-0749
[22] Gao Y, Checkel MD. Emission factors analysis for multiple vehicles using an on-board, in-use emissions measurement system. SAE Technical Papers 2007-01-1327, 2007(724), 776-790. https://doi.org/10.4271/2007-01-1327
[23] Bera P. Torque characteristic of SI engine in dynamic operating states. Combustion Engines. 2017;171(4):175-180. https://doi.org/10.19206/CE-2017-429
[24] Wendeker M, Jakliński P, Czarnigowski J. Experimental analysis of automotive engine conditions of operation. Eksploat Niezawodn. 2000;6:19-28.
[25] Aviation Artur Trendak TERCEL Carbon RSTi aircraft maintenance manual TERCEL-C-AMM-001-EN, edition 1. 28 Oct 2020.
[26] Boriboonsomsin K, Durbin T, Scora G, Johnson K, Sandez D, Vu A, et al. Real-world exhaust temperature and engine load distributions of on-road heavy-duty diesel vehicles in various vocations. Data Brief. 2018;18:1520-1543. https://doi.org/10.1016/j.dib.2018.04.044

Jacek Czarnigowski, DSc., DEng. – Faculty of Mechanical Engineering, Lublin University of Technology, Poland.
e-mail: *j.czarnigowski@pollub.pl*

Michał Trendak, MEng. – Faculty of Mechanical Engineering, Lublin University of Technology, Poland.
e-mail: *michal@trendak.eu*